Ab initio study of low-energy electron-methane scattering

B. H. Lengsfield III and T. N. Rescigno
Lawrence Livermore National Laboratory, P.O. Box 808, Livermore, California 94550

C. W. McCurdy
Department of Chemistry, Ohio State University, Columbus, Ohio 43210
(Received 15 November 1990)

The complex Kohn method is used to study electron-methane scattering with polarized trial functions at incident energies ranging from 0.2 to 10 eV. A perturbative method, which only requires the construction of Fock operators, is used to generate a set of polarized virtual orbitals. These polarized orbitals are then used to construct a compact *ab initio* scattering function that produces cross sections that are in excellent agreement with experiments in the region of the Ramsauer-Townsend minimum and at higher energies, where a broad maximum is present in the integral cross section. This is the first *ab initio* study to accurately characterize low-energy electron-methane scattering.

PACS number(s): 34.80.Gs

I. INTRODUCTION

The scattering of low-energy electrons from methane has been the subject of numerous theoretical studies in recent years [1–9]. These theoretical studies have focused on two distinct features of the cross section, the Ramsauer-Townsend (RT) minimum at 0.4 eV and a broad maximum at 8 eV. These features have been well characterized by several experimental efforts [10–14]. Electron-methane scattering provides a sensitive test of theory since a balance of exchange repulsion and polarization interactions is required to describe the Ramsauer minimum in the total cross section. Previous *ab initio* studies have established that static-exchange calculations alone are incapable of producing a RT minimum [8,9]. Since methane is the target gas in a variety of high-speed switching devices [15,16], a number of the theoretical studies were motivated by practical as well as purely academic considerations. Methane has also been used as a test bed for single-center scattering methods which employ model exchange and polarization potentials; more recently it has been the subject of *ab initio* calculations. Of the model potential studies, the most complete is that of Jain [2], who reports cross sections from 0.1 to 50 eV and presents an extensive set of differential cross sections. In these calculations, a parameter-dependent polarization potential is used to fix the RT minimum at the experimentally observed position and is then employed for incident energies below 1.0 eV. Electron-methane scattering has also been studied by Gianturco and Scialla [3] and by Yuan [5,6] using single-center scattering methods but with parameter-free polarization-correlation potentials of the Padial-Norcross [17] and O'Connell-Lane variety [18]. Yuan [6] has also compared single-center exact exchange calculations with the modified semiclassical exchange method developed by Gianturco and Scialla [3].

The calculations of Gianturco and Scialla produced a RT minimum at an energy very close to the experimental minimum. However, they did not report differential cross sections (DCS) in their work, and their integral cross section is not quantitative at low energies. Similar integral cross sections were obtained by Yuan, who also employed a single-center scattering method. Yuan computed differential cross sections at energies ranging from 3 to 20 eV. The DCS's reported by Yuan were in qualitative accord with experiment but significant quantitative differences were evident at 3, 5, and 6 eV.

The only previous *ab initio* study which attempted to include polarization effects was that of Lima, Watari, and McKoy [7], which used the multichannel Schwinger (MCS) method. The MCS studies were originally conducted at the static-exchange level [8] and later repeated [7] with the inclusion of closed channels to describe target polarization. The polarized MCS calculations did produce a Ramsauer minimum but at too low an energy. The discrepancy was attributed to the limited number of terms that were included in the configuration-interaction expansion they used to describe the closed channels.

In this study we employ the complex Kohn method [19,20] to study low-energy electron-methane scattering. Closed channels are included in the calculation to represent polarization of the target. A set of polarized virtual orbitals is generated by perturbation theory and is used to provide a compact representation of the closed channels included in the Kohn trial function. These compact trial functions are used to obtain differential and integral cross sections at incident electron energies ranging from 0.2 to 10 eV.

In Sec. II a brief review of the complex Kohn method is presented in order to develop a clear picture of how polarization is incorporated into the calculations. The procedure used to generate the polarized virtual orbitals will also be developed at this point. Section III provides a description of the Gaussian basis sets and wave functions employed in the current study as well as a discussion of our results. Section IV summarizes and concludes the paper.

II. THEORY

A. Polarization in the complex Kohn method

In the complex Kohn method we use a trial function of the form

$$\Psi_{\Gamma_0}(r_1,r_2,\ldots,r_{N+1})=\sum_{\Gamma}\mathcal{A}[\chi_\Gamma(r_1,r_2,\ldots,r_N)\times F_{\Gamma\Gamma_0}(r_{N+1})]+\sum_{\mu}d_\mu^{\Gamma_0}\Theta_\mu(r_1,r_2,\ldots,r_{N+1}) \tag{1}$$

where

$$F_{\Gamma\Gamma_0}(\mathbf{r})=\sum_{l,m}[f_l^\Gamma(r)\delta_{ll_0}\delta_{mm_0}\delta_{\Gamma\Gamma_0}+T_{lml_0m_0}^{\Gamma\Gamma_0}g_l^\Gamma(r)]\times Y_{lm}(\hat{\mathbf{r}})/r+\sum_k c_k^{\Gamma\Gamma_0}\varphi_k^\Gamma(\mathbf{r})\ . \tag{2}$$

The first sum in Eq. (1) runs over the energetically open target states denoted by χ_Γ. These target states need not be restricted to a single configuration but may be configuration-interaction wave functions. The functions f_l^Γ and g_l^Γ behave asymptotically as linearly independent regular and outgoing Ricatti-Bessel functions, respectively,

$$\begin{aligned} f_l^\Gamma(r)&=\frac{h(r)j_l(k_\Gamma r)}{(k_\Gamma)^{1/2}}\sim\frac{\sin(k_\Gamma r-l\pi/2)}{(k_\Gamma)^{1/2}}\quad\text{as } r\to\infty\ ,\\ g_l^\Gamma(r)&=\frac{ih(r)[j_l(k_\Gamma r)+in_l(k_\Gamma r)c(r)]}{(k_\Gamma)^{1/2}}\\ &\sim\frac{\exp[i(k_\Gamma r-l\pi/2)]}{(k_\Gamma)^{1/2}}\quad\text{as } r\to\infty\ . \end{aligned} \tag{3}$$

The functions $h(r)$ and $c(r)$ are cutoff factors, $c(r)$ being chosen to ensure that g_l^Γ is regular at the origin and $h(r)$ chosen to further exclude both the regular and outgoing wave continuum functions from the region near the origin. We define these functions as

$$\begin{aligned} c(r)&=(1-e^{-\alpha r})^{(2l+1)}\ ,\\ h(r)&=(1-e^{-\gamma r})^{(n)}\ . \end{aligned} \tag{4}$$

The channel momenta arising in these expressions are determined by energy conservation:

$$k_\Gamma=[2(E-E_\Gamma)]^{1/2}\quad\text{for } E>E_\Gamma\ . \tag{5}$$

The Kohn trial function also contains square-integrable (L^2) one-electron functions, φ_k^Γ, which are distinct from the L^2 functions used to build the target wave functions, and a sum of L^2 $(N+1)$-electron configuration state functions, Θ_μ.

The continuum functions g_l^Γ and f_l^Γ are orthogonalized to *all* of the L^2 functions employed in the Kohn trial wave function. This orthogonalization is dictated by practical considerations involving the evaluation of Hamiltonian matrix elements. It also allows us to eliminate an entire class of bound-free and free-free matrix elements by using separable expansions to approximate certain parts of the interaction potential. The orthogonalization of the continuum functions f_l^Γ and g_l^Γ to the scattering functions φ_k^Γ simply represents a unitary transformation of the total wave function which leaves the T matrix unchanged. The orthogonalization of the continuum functions to the L^2 functions comprising the target wave function, however, can represent an unphysical constraint in the calculation which must be relaxed by inclusion of appropriate configurations in the set $\{\Theta_\mu\}$. If not relaxed, this orthogonalization restricts the penetration of the target by the incident electron. Orthogonality relaxing configurations which remove these constraints are generated by taking the direct product of the target wave function and an occupied orbital. For example, a two-electron target wave function, $\Psi_T=\sigma_1\sigma_2$, would give rise to the orthogonality relaxing configurations $\sigma_1^2\sigma_2$ and $\sigma_1\sigma_2^2$ when the doublet contribution to the cross section is computed.

Polarization of the target by the incident electron is an important effect at low energies. To incorporate this effect into the calculation in an *ab initio* fashion, we must include closed channels in the Kohn wave function. One way to accomplish this would be to generalize the trial wave function to the form

$$\Psi_{\Gamma_0}=\sum_{\Gamma}^{\text{open,closed}}\mathcal{A}\chi_\Gamma(r,\ldots,r_N)F_{\Gamma\Gamma_0}(r_{N+1})+\sum_\mu d_\mu^{\Gamma_0}\Theta_\mu^{\Gamma_0}(r_1,\ldots,r_{N+1}) \tag{6}$$

with

$$\int\chi_\Gamma\mathcal{H}\chi_{\Gamma'}=\delta_{\Gamma\Gamma'}E_\Gamma \tag{7}$$

where the channel functions corresponding to closed channels are now expanded as

$$F_{\Gamma\Gamma_0}^{\text{closed}}(r)=\sum_k c_k^\Gamma\varphi_k(r)+\sum_{l,m}c_{lm}^\Gamma i_{lm}^\Gamma(r)Y_{lm}(\hat{\mathbf{r}})/r \tag{8}$$

with

$$i_{lm}^\Gamma(r)\sim\exp\{-[2(E_\Gamma-E_{\Gamma'})]^{1/2}\}r\quad\text{as } r\to\infty\ . \tag{9}$$

An alternate approach, which is the one we have adopted here, is to make use of the fact that all closed-channel contributions to Ψ_Γ fall off exponentially as any electron coordinate tends to infinity. The closed-channel contribution to Ψ_{Γ_0} can thus be incorporated into Eq. (1) by the inclusion of appropriate $(N+1)$-electron configurations in $\{\Theta_\mu\}$, which are the direct product of closed-channel wave functions and the square-integrable functions φ_k. As the set of square-integrable one-electron functions φ_k approaches completeness, the two formulations become equivalent. Thus, in the formulation we have used here, the $(N+1)$-electron terms $\{\Theta_\mu\}$ not only contain the "penetration terms" needed to remove orthogonality constraints from the calculation, but also contain terms needed to describe polarization and correlation effects not accounted for in the first term in Eq. (1).

If we were to adopt the alternative method of incorporating closed channels by retaining the exponentially decaying functions and moving the closed-channel target wave functions into P space, the occupied orbitals in these closed channels could no longer be included in the sum over square-integrable functions present in the one-electron scattering function $F_{\Gamma\Gamma_0}$ defined in Eq. (2). In the absence of a separable approximation, such a repartitioning of the scattering problem would not affect the outcome of the calculations. Since we do invoke separable approximations, it is advantageous to retain these square-integrable functions in $F_{\Gamma\Gamma_0}$. For this reason, we included the closed-channel wave functions in Q space and we did not adopt this P-space formulation of the problem.

The T-matrix elements appearing in Eq. (2) determine the electron scattering cross sections and are obtained by requiring that the Kohn functional

$$[T^{\Gamma\Gamma_0}]=T^{\Gamma\Gamma_0}-2\int \Psi_\Gamma(\mathcal{H}-\mathcal{E})\Psi_{\Gamma_0} \tag{10}$$

be made stationary. This leads to a set of linear equations for the variational parameters, $T^{\Gamma\Gamma_0}$, $C_R^{\Gamma\Gamma_0}$ and $d_\mu^{\Gamma_0}$, present in the Kohn trial function. In practice, the second sum in Eq. (1) can be formally eliminated by using Feshbach partitioning to define an effective Hamiltonian. Denoting the two parts of Ψ_{Γ_0} in Eq. (1) as $P\Psi_{\Gamma_0}$ and $Q\Psi_{\Gamma_0}$, we find that $P\Psi_{\Gamma_0}$ satisfies a Schrödinger equation with the effective Hamiltonian

$$\begin{aligned}\mathcal{H}_{\text{eff}}&=\mathcal{H}_{pp}-\mathcal{H}_{pq}(\mathcal{H}_{qq}-E)^{-1}\mathcal{H}_{qp}\\&=\mathcal{H}_{pp}+V_{\text{opt}}\ .\end{aligned} \tag{11}$$

Thus the optical potential V_{opt} appearing in this expression for the effective Hamiltonian $\mathcal{H}_{\text{eff}}$ contains contributions from both polarization and orthogonality relaxing $(N+1)$-electron terms. The stationary expression for the T matrix is found to be [21]

$$[T]=-2(M_{00}-M_{q0}^t M_{qq} M_{q0}) \tag{12}$$

where the matrix elements of M are obtained from the operator $(\mathcal{H}_{\text{eff}}-E)$. The subscript 0 denotes the functions $\{\chi_\Gamma f_l^\Gamma Y_{lm}\}$ and the subscript q denotes the subspace spanned by the functions $\{\chi_\Gamma g_l^\Gamma Y_{lm}\}$ and $\{\chi_\Gamma \varphi_k^\Gamma\}$.

In these calculations, separable exchange and separable optical potential approximations were invoked. The separable exchange approximation results in the elimination of exchange integrals involving continuum functions from $\mathcal{H}_{pp}$ [22]. The direct integrals involving continuum functions which contribute to $\mathcal{H}_{pp}$ are evaluated by an adaptive quadrature procedure developed by McCurdy and Rescigno [9]. The separable optical approximation results in a real-valued optical potential as the elements of $\mathcal{H}_{pq}$ which involve continuum functions are zero. The optical potential can then be evaluated solely with electronic structure codes. Both of these approximations assert that the L^2 portion of the scattering basis, represented by the sum over φ_k^Γ in Eq. (2), approaches a complete set of functions and thus is large enough to account for these interactions. Thus we have

$$\begin{aligned}\mathcal{H}_{qp}|f_l Y_{lm}\rangle&=\sum_n^\infty \mathcal{H}_{qp}|\phi_n\rangle\langle\phi_n|f_l Y_{lm}\rangle\\&\cong\sum_k \mathcal{H}_{qp}|\varphi_k\rangle\langle\varphi_k|f_l Y_{lm}\rangle\\&=0\end{aligned} \tag{13}$$

since

$$\langle\varphi_k|f_l Y_{lm}\rangle=0 \tag{14}$$

as a result of orthogonalizing the continuum functions to the L^2 functions. Equations (13) and (14) also hold for the outgoing continuum functions g_l. In Eq. (13), $\{\phi_\mu\}$ represents a complete set of one-electron functions and $\{\varphi_k\}$ are again the L^2 functions which appear in the Kohn trial function. Thus Q space, which contains the polarization terms in these calculations, is only coupled to P space via the square-integrable functions φ_k present in $F(r)$ of Eq. (1).

In order to obtain a compact trial function, the Hartree-Fock virtual orbitals are subjected to a transformation which splits the virtual space into a small number of polarized virtual orbitals and a complementary set of virtual orbitals. The molecular polarizability computed from the closed channels defined in terms of these polarized orbitals is equivalent to that obtained by employing the full set of virtuals to first order in perturbation theory. The transformation used to define these polarized virtual orbitals is described in the next section. In our calculations we employ a single configuration, Hartree-Fock target wave function and represent closed channels by single excitations into the polarized orbital space. The configurations employed in the Kohn trial function would then be generated by the electron distributions found in Table I. All configuration state func-

TABLE I. Electron distributions used to define the target states and the Kohn trial wave functions.

Orbital space	Valence	Polarized	Virtual
Hartree-Fock target	8	0	0
Closed channels	7	1	0
Trial P space	8	1	0
	8	0	1
Trial Q space	7	2	0
	7	1	1

tions of the appropriate spin and spatial symmetry arising from these electron distributions would be retained. These distributions include closed-channel configurations of different spin and spatial symmetry from that of the target wave function. The importance of these polarization terms has been previously noted by Schneider and Collins [23] and by Lima, Watari, and McKoy [7].

Before considering the results of our calculations, we need to examine the structure of our trial Kohn function in greater detail. The configurations that were introduced in Q space to describe the target polarization and to relax orthogonality constraints must not introduce N-electron correlation terms in the Kohn trial function that were not present in the target wave function. These spurious terms would result in an unphysical optical potential that was much too attractive. Equation (7) is a necessary but not sufficient condition to ensure that these recorrelation terms are absent from the Kohn trial function. We have avoided this problem by employing the direct-product configurations mentioned previously and illustrated in Table I. However, the design of a trial function which yields a balanced description of N- and $(N+1)$-electron interactions needed to obtain reliable cross sections near the Ramsauer-Townsend minimum is a more formidable undertaking. A polarized-self-consistent-field (SCF) trial function was used by Schneider and Collins [23] to study the shape resonance in N_2 and this function was found to "overpolarize" the target if the full virtual space was employed in the construction of the $(N+1)$-electron configurations. This imbalance between the N-electron and the $(N+1)$-electron wave functions arises because the configuration state functions which were introduced to polarize the target can also introduce correlation in the $(N+1)$-electron wave function. The analogous correlation terms do not exist in the N-electron target wave function. This imbalance will persist unless full configuration-interaction (CI) wave functions, in which the same orbital space is used to represent the target and closed channels, are used in the calculations. One would expect this imbalance to diminish as one introduces increasing levels of correlation in the target wave function. This effect is well known and has been addressed in the past by employing semiempirical cutoff parameters in scattering calculations which employ model polarization potentials.

In order to investigate this effect, the virtual orbital space was partitioned yet again and trial wave functions generated from the electron distributions shown in Table II were investigated. These polarized Kohn trial functions can be uniquely defined by a set of three numbers (a,b,c), which indicate the number of virtual orbitals contained in each partition. The results of these studies will be presented in the discussion section of this work.

It is well known that a large number of partial waves are needed to converge the elastic electron scattering cross section of a polarizable target. However, the higher partial-wave contributions need not be explicitly computed in the Kohn calculations as they can be obtained from a partial-wave Born approximation with a spherically averaged effective Hamiltonian [24]. Expressions for the phase shifts η_l^{Born} and scattering amplitudes in this approximation were developed by Thompson [25] and O'Malley, Spruch, and Rosenberg [26].

$$\tan\eta_l^{\text{Born}}=\frac{\pi\alpha_d k^2}{(2l+3)(2l+1)(2l-1)},\quad l>0\ , \tag{15}$$

$$f(\Theta)=\frac{1}{k}\left[\sum_{l=0}^{2}(2l+1)e^{i\eta_l}\sin\eta_l P_l(\cos\theta)+\sum_{l=3}^{\infty}(2l+1)e^{i\eta_l^{\text{Born}}}\sin\eta_l^{\text{Born}}P_l(\cos\theta)\right]$$
$$=\frac{1}{k}\sum_{l=0}^{2}(2l+1)e^{i\eta_l}\sin\eta_l P_l(\cos\theta)+\pi\alpha_d k\left[\frac{1}{3}-\frac{1}{2}\sin\frac{\theta}{2}-\sum_{l=1}^{2}\frac{P_l(\cos\theta)}{(2l+3)(2l+1)}\right] \tag{16}$$

TABLE II. Electron distributions used to generate the Kohn trial function and target states with a repartitioned virtual space. The distributions are uniquely defined by the notation (a,b,c), which refers to the number of orbitals in each partition of the virtual space.

Orbital space	Valence orbitals	a Polarized orbitals	b Virtual orbitals	c Virtual orbitals
Hartree-Fock target	8	0	0	0
Closed channels	7	1	0	0
Trial P space	8	1	0	0
	8	0	1	0
	8	0	0	1
Trial Q space	7	2	0	0
	7	1	1	0

where α_d is the polarizability of the target. The differential and integral cross sections are given as

$$\frac{d\sigma}{d\Omega}=|f(\Theta)|^2 , \tag{17}$$

$$\sigma_I=\frac{4\pi}{k^2}\sum_{l=0}^{2}(2l+1)\sin^2\eta_l+\frac{\pi^3\alpha_d^2k^2}{2450} . \tag{18}$$

It is important to bear in mind that these expressions are also used to extrapolate experimental differential cross sections to scattering angles near 0° and 180° [14]. In our work, we only employ these formulas to account for partial-wave contributions with $l>2$.

B. Polarized orbitals

The notion of a polarized orbital in scattering calculations is usually associated with the polarized orbital method of Callaway *et al.* [27,28] and Temkin and Lamkin [29,30]. In this method, an adiabatic approximation is used to treat the interaction of the incident electron with the target. The response of a Hartree-Fock orbital to an external field is represented, to first order in perturbation theory, as the sum of a Hartree-Fock orbital and a polarized orbital,

$$\varphi_1=\varphi_0+\varphi_P . \tag{19}$$

An iterative procedure is then employed to obtain the polarized orbital at a variety of electron-target separations. These orbitals are then used to define static and polarization potentials employed in the scattering calculations. Polarized orbitals have also been used by Schneider and Collins [23] as efficient means of incorporating target polarization in their linear-algebraic studies of N_2 resonances. In the Schneider-Collins treatment, a single Hartree-Fock calculation was performed with an electric field present. These Hartree-Fock orbitals were then orthogonalized to the zero-field orbitals to yield the polarized orbitals.

In this work we employ perturbation theory to define a set of polarized orbitals. We chose a formalism where each valence orbital is independently perturbed by an external dipole field. This allows us to employ only one-electron, Fock-like operators in our expressions. There will be three polarized orbitals, one generated by each component of the dipole operator, for each occupied valence orbital. The virtual orbitals are first rotated by a V_{N-1} Fock operator, where the hole is placed in the orbital that is being polarized, to generate a set of improved virtual orbitals (IVO's). A basis of singly excited configuration state functions could then be generated by exciting the orbital we wish to polarize. In this basis, the Hamiltonian is diagonal and the first-order wave function is obtained from

$$\Psi_1^\alpha=\sum_{i\neq 0}\frac{|\Psi_i\rangle\langle\Psi_i|\mu_\alpha|\Psi_0\rangle}{E_i-E_0} \tag{20}$$

where Ψ_0 is the Hartree-Fock wave function, μ_α is a component of the dipole operator, Ψ_i is a configuration state function (CSF) generated by singly exciting the valence orbital that is to be polarized, E_i is the energy of this singly excited CSF, and E_0 is the Hartree-Fock energy. Since we polarize only one occupied orbital at a time, this expression for a first-order wave function reduces to an expression for a perturbed orbital,

$$\varphi_1^\alpha=\sum_{i}^{\text{virtual}}\frac{|\varphi_i\rangle\langle\varphi_i|\mu_\alpha|\varphi_0\rangle}{\varepsilon_i-\varepsilon_0} \tag{21}$$

where ε_i is the ith eigenvalue of the singlet IVO or V_{N-1} Fock operator,

$$\mathcal{F}_{\text{IVO}}=h+2J_C-K_C+J_0+K_0 \tag{22}$$

and ε_0 is the closed-shell Hartree-Fock eigenvalue of the orbital that is being polarized. In Eq. (22), h is the sum of one-electron kinetic energy and electron nuclear attraction operators, J_C and K_C are the Coulomb and exchange operators for the core (doubly occupied) orbitals, and J_0 and K_0 are the Coulomb and exchange operators for the orbital being polarized. This procedure is repeated for each occupied orbital and then the resulting polarized virtual orbitals are orthogonalized. A compact representation of the closed channels used to account for target polarization in the Kohn trial functions are generated by singly exciting the valence, occupied orbitals into the space of polarized virtual orbitals.

In practice, it was convenient to obtain these orbitals by diagonalizing the following operator in the space of IVO functions, φ_i:

$$P_{ij}^\alpha=\frac{\langle\varphi_i|\mu_\alpha|\varphi_0\rangle\langle\varphi_0|\mu_\alpha|\varphi_j\rangle}{(\varepsilon_i-\varepsilon_0)(\varepsilon_j-\varepsilon_0)} \tag{23}$$

which is derived by optimizing the square of the first-order interaction subject to orthogonality constraints. P_{ij}^α is a rank-one operator whose single eigenvector with a nonzero eigenvalue is the polarized orbital in question. By using standard diagonalization techniques, all of the orbitals in a degenerate shell could be treated at one time and the resulting polarized orbitals could be constrained to transform as irreducible representations of both the T_d and C_{2v} point groups. This operator is analogous to the operator used by Amos and Hall [31] to define corresponding orbitals in unrestricted Hartree-Fock (UHF) theory and to the operator employed by Foster and Boys [32] to generate oscillator orbitals. The operator used by Foster and Boys differs from that defined in Eq. (23) by the absence of the terms in the denominator.

We have tested this procedure by comparing the polarizability computed in the polarized orbital space to that obtained by using the full virtual space and we found the results agreed to better than 2%. Oscillator orbitals were also investigated in these calculations and were found to yield much poorer results. The results of these tests are reported in the next section where the calculations are described in detail.

The complementary set of virtual orbitals ought to be uniquely defined as it is often desirable to employ a subset of these orbitals in the polarized-Kohn trial function. These orbitals were uniquely defined by diagonalizing a V_{N-1} Fock operator in this orbital space.

This procedure can be readily generalized to polarize open-shell Hartree-Fock or multiconfiguration self-consistent-field (MCSCF) target wave functions by using coupled perturbed Hartree-Fock [33] or multiconfiguration coupled-perturbed Hartree-Fock [34,35] theory to generate the polarized orbitals. These techniques are routinely used in electronic structure theory [36] to extract the dipole moment from a correlated wave function or to differentiate Born-Oppenheimer energy expressions with respect to the position of the atoms. These techniques allow us to define a hierarchy of polarized target wave functions that can be employed in scattering calculations using a series of MCSCF wave functions to describe the target. This technique can also be used to design a compact contracted basis set which yields an optimum value of a molecular property.

TABLE III. Gaussian basis sets.

Hydrogen [6*s*1*p*/3*s*1*p*] core basis		Carbon [12*s*6*p*/8*s*4*p*] core basis			
Type *S*		Type *S*		Type *P*	
74.69	0.025 374	4232.61	0.006 228	18.155 70	0.039 196 0
11.23	0.189 684	634.882	0.047 676	3.986 40	0.244 144
2.546	0.852 933	146.097	0.231 439	1.142 90	0.816 775
		42.497 4	0.789 108		
0.7130	1.0			0.359 40	1.0
		14.189 20	0.791 751		
0.2249	1.0	1.966	0.321 87	0.114 60	1.0
Type *P*					
0.75	1.0	5.147 7	1.0	0.05	1.0
		0.496 20	1.0		
		0.153 30	1.0		
		0.05	1.0		
		0.02	1.0		
		0.01	1.0		

Basis *A* Core [C:2*d*]		Basis *B* Core [C:1*p*3*d*]		Basis *C* Core [H:1*s*,C:1*s*2*p*5*d*]		Basis *D* Core [H:1*s*1*p*,C:1*s*2*p*5*d*]	
Hydrogen							
None		None		Type *S*		Type *S*	
				0.08	1.0	0.08	1.0
						Type *P*	
						0.32	1.0
Carbon							
Type *D*		Type *P*		Type *S*		Type *S*	
1.097	1.0	0.02	1.0	0.004	1.0	0.004	1.0
		Type *D*		Type *P*		Type *P*	
0.318	1.0	0.75	1.0	0.02	1.0	0.02	1.0
		0.09	1.0	0.007	1.0	0.007	1.0
		0.035	1.0				
				Type *D*		Type *D*	
				1.097	1.0	1.097	1.0
				0.318	1.0	0.318	1.0
				0.09	1.0	0.09	1.0
				0.035	1.0	0.035	1.0
				0.01	1.0	0.01	1.0

Polarizability (α_0)			
Polarized orbitals			
15.32	17.49	17.74	17.98
Full virtual space			
15.47	17.70	17.98	18.22

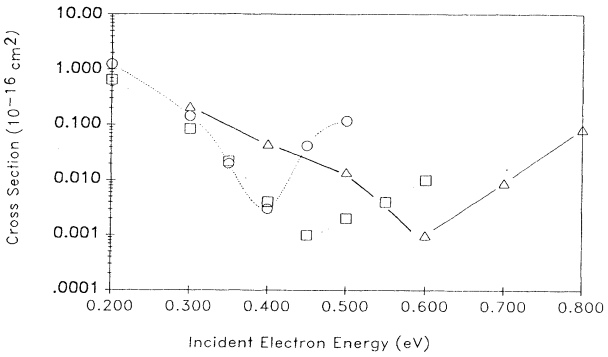

FIG. 1. Partial cross sections in A_1 symmetry obtained with basis sets B (circles), C (squares), and D (triangles).

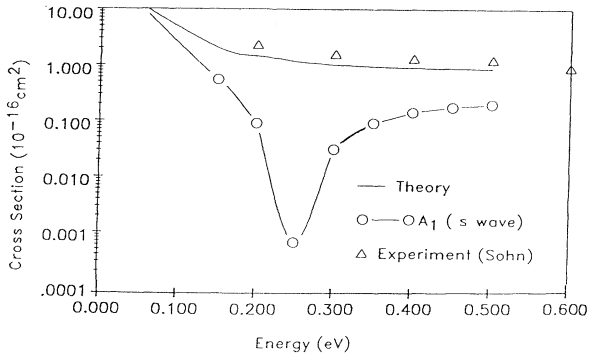

FIG. 3. Low-energy cross sections obtained from the (12,39,29) trial function.

III. RESULTS AND DISCUSSION

In this section we present integral and differential cross sections obtained in our complex Kohn calculations at incident electron energies ranging from 0.1 to 10 eV. The results of polarized-SCF calculations will be discussed in light of the earlier theoretical work of Lima, Watari, and McKoy [7], and Jain [1], as well as the recent experimental work of Sohn *et al.* [14], Lohmann and Buckmann [13], and Ferch, Granitza, and Raith [11]. In order to ensure that converged cross sections were obtained in the polarized-SCF calculations, a series of Gaussian basis sets were employed to describe the target wave function and the L^2 portion of the Kohn scattering function [Eq. (2)]. These basis sets are given in Table III. Basis sets $A-D$ are defined by augmenting a core hydrogen-carbon Gaussian basis. At the bottom of this table, the symmetric polarizability α_0 obtained with these basis sets is reported. The polarizability was computed as a sum over states from SCF plus singles CI wave functions, the same

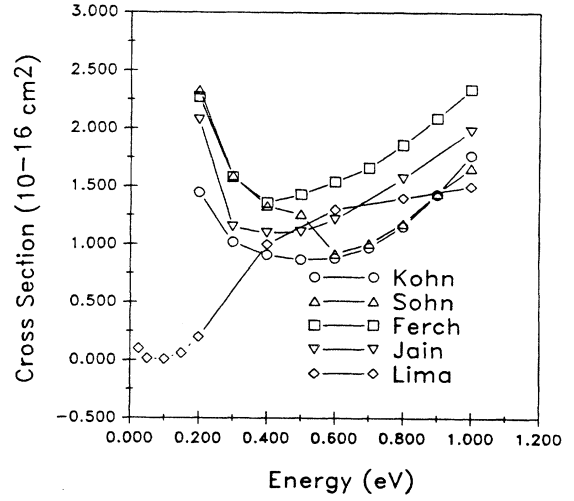

FIG. 4. Comparison of experimental and theoretical integral cross sections below 1.0 eV.

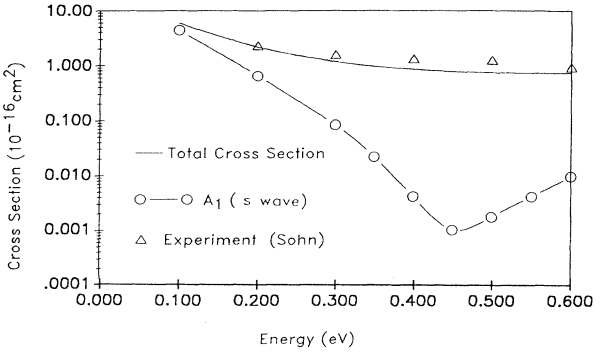

FIG. 2. Low-energy cross sections obtained from the (12,61,7) trial function.

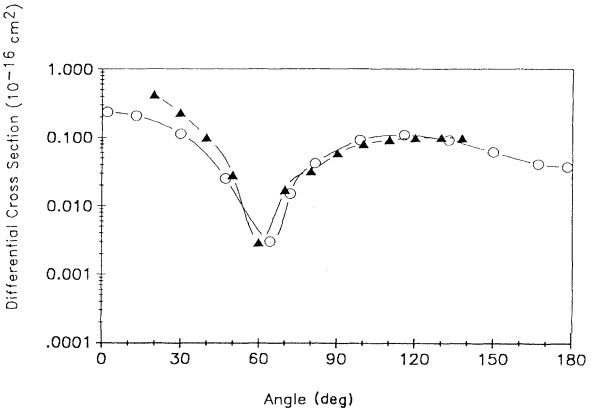

FIG. 5. Differential cross section at 0.5 eV obtained from the (12,39,29) trial function. ○ — ○, present results. ▲ — ▲, experiments of Sohn *et al.* [14].

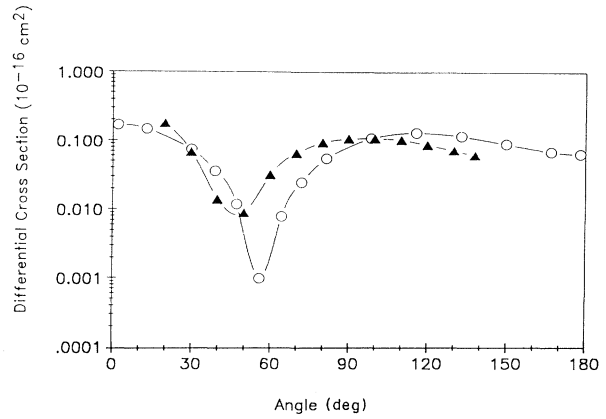

FIG. 6. Differential cross section at 0.7 eV obtained from the (12,39,29) trial function. ○ — ○, present results. ▲ — ▲, experiments of Sohn *et al.* [14].

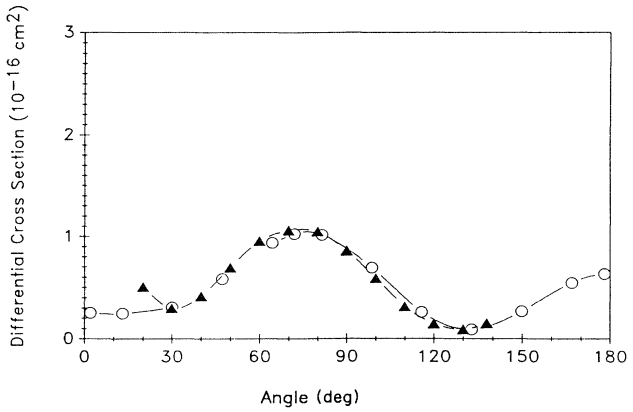

FIG. 8. Differential cross section at 3.0 eV obtained from the (12,39,29) trial function. ○ — ○, present results. ▲ — ▲, experiments of Sohn *et al.* [14].

wave functions that were used to represent closed channels in the scattering trial functions. Polarizability calculations were conducted using the full virtual space and also using only the polarized virtual orbitals. We found that the polarized virtual orbitals in CH_4 were insensitive to the spin coupling employed in the IVO Fock operator [see Eq. (22)] and triplet IVO's were employed in the algorithm used to generate the polarized virtual orbitals. The results obtained from these two sets of calculations agree to better than 2% and basis sets *B* and *C* agree well with the experimental value of $17.5a_0^3$. In Fig. 1, the A_1 partial cross sections obtained with the basis sets *B*–*D* are plotted. As seen in this figure, the location of the Ramsauer minimum moves to higher scattering energies with increasing polarizability. In all of these calculations, polarized virtual orbitals were employed in Kohn trial functions of type $(12,n_v-19,7)$ where n_v is the number of virtual orbitals in each basis. This type of

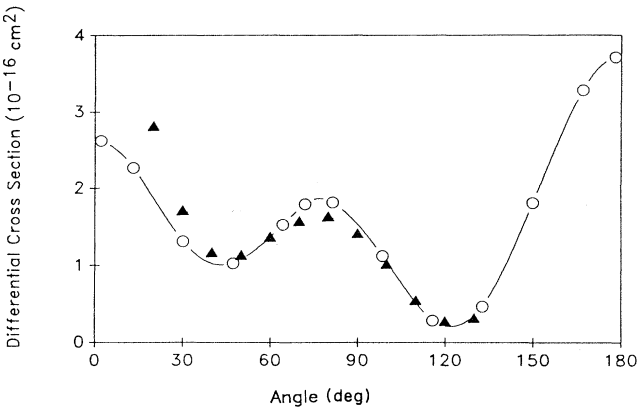

FIG. 9. Differential cross section at 5.0 eV obtained from the (12,39,29) trial function. ○ — ○, present results. ▲, experiments of Sohn *et al.* [14].

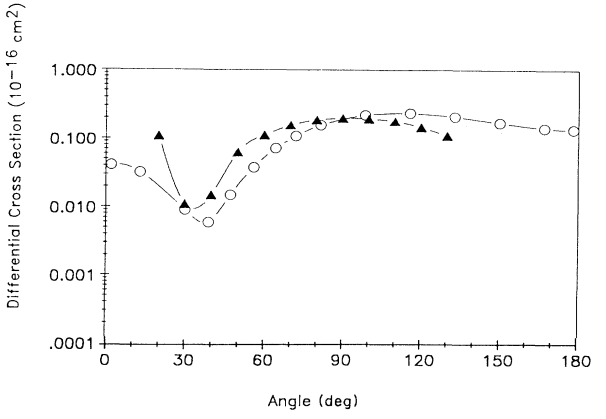

FIG. 7. Differential cross section at 1.0 eV obtained from the (12,39,29) trial function. ○ — ○, present results. ▲ — ▲, experiments of Sohn *et al.* [14].

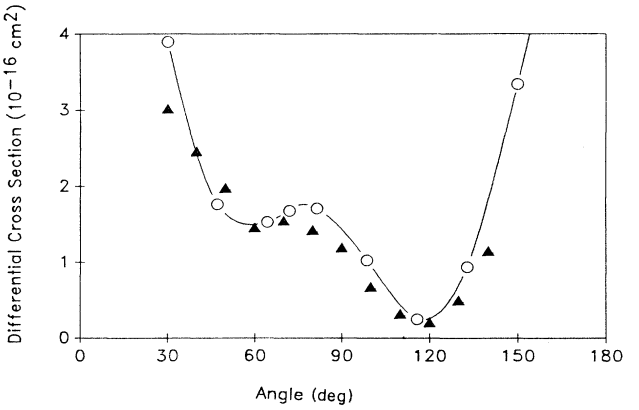

FIG. 10. Differential cross section at 7.5 eV obtained from the (12,39,29) trial function. ○ — ○, present results. ▲, experiments of Sohn *et al.* [14].

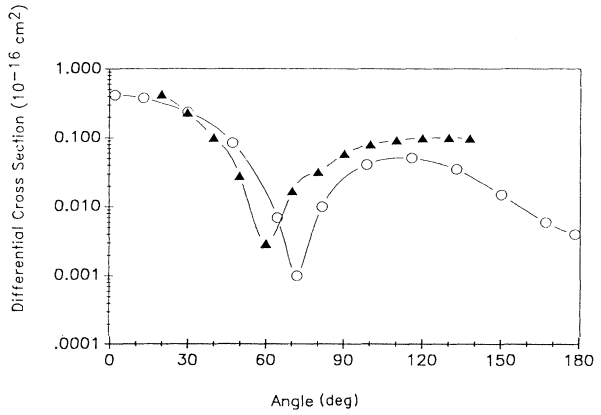

FIG. 11. Differential cross section at 0.5 eV obtained from the (12,61,7) trial function. ○ — ○, present results. ▲ — ▲, experiments of Sohn *et al.* [14].

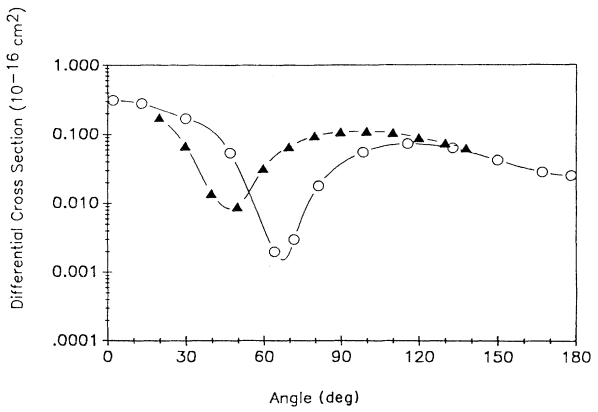

FIG. 12. Differential cross section at 0.7 eV obtained from the (12,61,7) trial function. ○ — ○ present results, ▲ — ▲, experiments of Sohn *et al.* [14].

scattering function was discussed in the preceding section and depicted in Table II. In the basis sets employed in this work, seven orbitals were found to possess IVO eigenvalues greater than 6.9 hartrees and were excluded from the Q-space portion of the Kohn trial function. Orbitals with eigenvalues of this magnitude have a negligible effect on the calculated optical potential.

An additional calculation was also performed using basis D to investigate the sensitivity of these results to the separable exchange and separable optical potential approximations employed. This calculation was also undertaken to support the notion that the position of the Ramsauer minimum in our calculations is a function of the target polarizability. As seen in Table III, basis C and basis D differ only by the addition of a p function on hydrogen. In this additional calculation, the polarized virtual orbitals were defined in basis C and then the additional p function was included in the square-integrable portion of the scattering basis. Thus the target polarizability is equal to that of basis C and the separable approximations are treated at the same level as in the basis D calculations. The results of this calculation and the previous basis-set studies are given in Table IV. We found

TABLE IV. Low-energy A_1 partial cross sections. Cross-section units are 10^{-16} cm^2.

	Basis			
Energy (eV)	*B*	*C*	*D*	*E*
0.200	1.246	0.650		0.646
0.300	0.143	0.084	0.212	0.083
0.350	0.020	0.022		
0.400	0.003	0.004	0.045	0.003
0.450	0.042	0.001		
0.500	0.117	0.002	0.014	0.001
0.550		0.004		
0.600		0.010	0.001	0.008
0.700			0.009	0.045
0.800			0.085	0.158

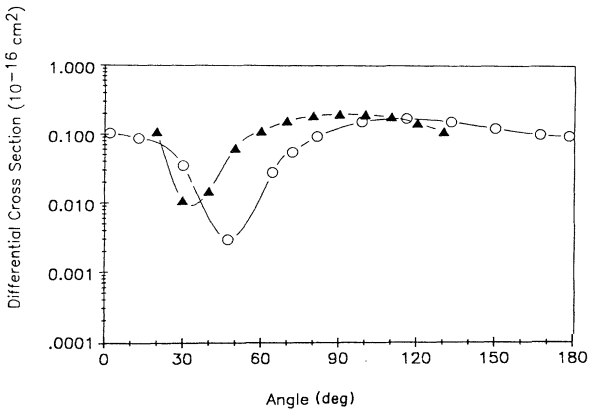

FIG. 13. Differential cross section at 1.0 eV obtained from the (12,61,7) trial function. ○ — ○, present results. ▲ — ▲, experiments of Sohn *et al.* [14].

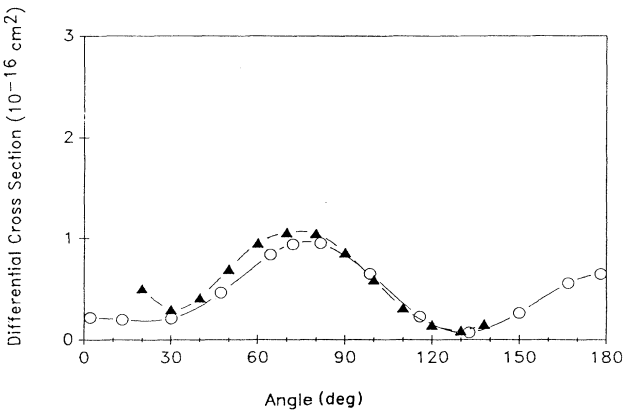

FIG. 14. Differential cross section at 3.0 eV obtained from the (12,61,7) trial function. ○ — ○, present results. ▲ — ▲, experiments of Sohn *et al.* [14].

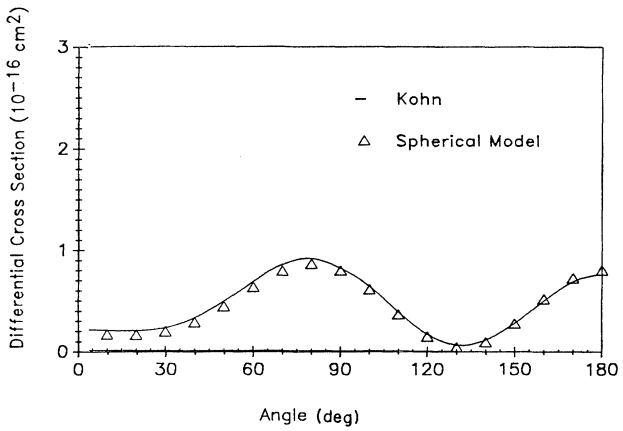

FIG. 15. Comparison of differential cross sections at 3.0 eV.

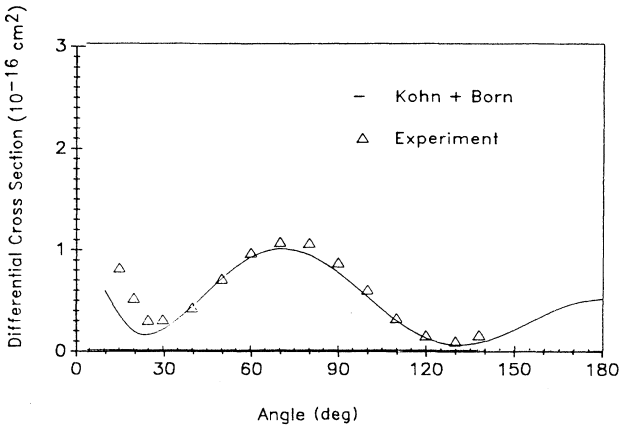

FIG. 17. Differential cross section at 3.0 eV with $l>2$ partial-wave contributions from the polarized-Born approximation. △, experiments of Sohn *et al.* [14].

that the results of this study, labeled basis *E* in Table IV, produce a Ramsauer minimum very near to that obtained from basis *C* which indicates that the shift in the minimum is not an artifact of the separable approximations but is a response to a change in target polarizability.

Other Kohn trial functions of the type $(12+m,n_v-19-m,7)$, which increases the number of virtual orbitals used to define closed channels in the optical potential, were also studied. These terms might also bias the $(N+1)$-electron terms in the trial wave function by introducing correlation terms not present in the SCF description of the *N*-electron target. This, in fact, is what was observed as the Ramsauer minimum shifted to significantly higher energies than found in the calculations which used only the polarized virtual orbitals to describe target polarizability.

These observations led us to employ compact, polarized-SCF trial functions in the scattering calculations where only polarized virtual orbitals were used to describe target polarizability and where the basis set was chosen to match the polarizability obtained either from experiment or, in general, from a large electronic structure calculation. This simple prescription allows us to achieve a reasonable balance between the *N*- and $(N+1)$-electron wave functions without resorting to a more elaborate CI description of the target. The polarizability obtained with basis *D* is too large. Basis *B* was found to yield a polarizability which was comparable to that found with basis *C*, but it was found that the *d*-wave contributions to the cross sections were not converged and thus the larger basis, basis *C*, was employed in our final calculations. The Kohn trial function we employed would then be denoted as (12,61,7). We also report the results of calculations obtained from a (12,39,29) trial

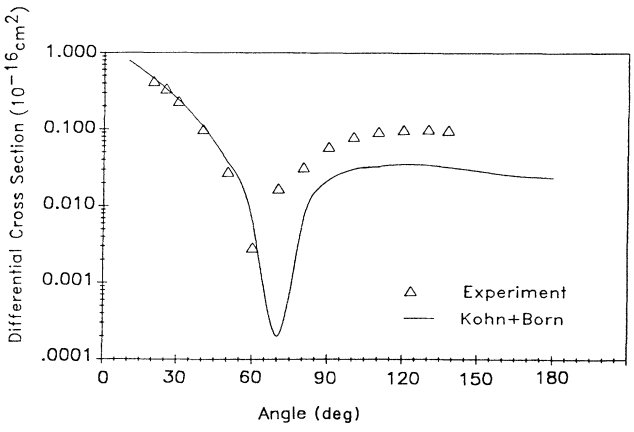

FIG. 16. Differential cross sections at 0.5 eV with $l>2$ partial-wave contributions from the polarized-Born approximation. △, experiments of Sohn *et al.* [14].

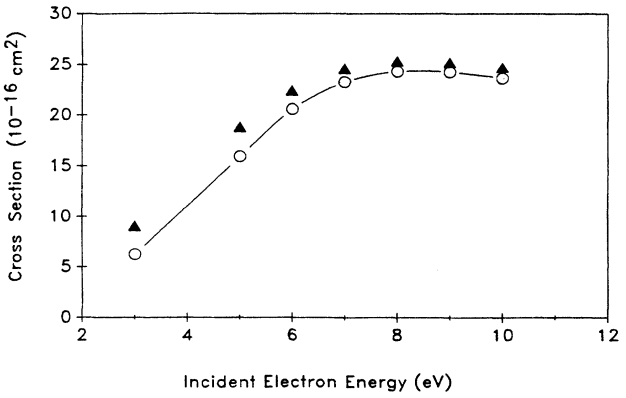

FIG. 18. Total cross section. ○—○, present results. ▲, experiments of Lohmann and Buckmann [13].

TABLE V. Differential cross sections obtained with (12,61,7) trial functions. Cross-section units are 10^{-16} cm^2.

Angle (deg)	0.5 eV	0.7 eV	1.0 eV	3.0 eV	5.0 eV	7.5 eV
2.000	0.417	0.314	0.103	0.219	2.622	7.812
13.118	0.377	0.282	0.087	0.197	2.269	6.856
30.110	0.235	0.170	0.035	0.210	1.312	3.897
47.202	0.084	0.054	0.003	0.463	1.031	1.765
64.317	0.007	0.002	0.028	0.838	1.579	1.534
72.000	0.001	0.003	0.055	0.941	1.796	1.679
81.438	0.010	0.018	0.094	0.951	1.820	1.710
98.562	0.041	0.055	0.153	0.650	1.125	1.027
115.683	0.051	0.073	0.172	0.226	0.284	0.249
132.798	0.035	0.063	0.155	0.069	0.465	0.941
149.890	0.015	0.042	0.125	0.263	1.811	3.340
166.882	0.006	0.028	0.102	0.555	3.284	5.850
178.000	0.004	0.025	0.097	0.645	3.714	6.579

function, where this scattering wave function was defined by truncating the virtual space at IVO eigenvalues less than 1.00, in order to assess the sensitivity of our results to orbital truncation. In these calculations, we included partial waves up to $l=5$. The calculations were performed in C_{2v} symmetry. The integral cross sections and s-wave partial cross sections obtained in these calculations are given in Figs. 2 and 3. The Ramsauer minimum shifts to lower energies with the truncated virtual space but the integral cross section was not significantly affected. In Fig. 4, integral cross sections below 1.0 eV are compared with the experimental work of Sohn *et al.* [14] and Ferch, Granitza, and Raith [11], the *ab initio* Schwinger calculations of Lima, Watari, and McKoy [7], and to the semiempirical calculations of Jain [1]. The crossed-beam work of Sohn *et al.* reports vibrationally elastic cross sections and produces a shoulder near the first vibrational threshold which is not present in the vibrationally inelastic work of Ferch, Granitza, and Raith. The agreement between the experimental results of Sohn *et al.* and the present theoretical results is very good in light of the simple, uncorrelated, target wave functions employed in our studies.

Differential cross sections at energies ranging from 0.5 to 7.5 eV are presented in Figs. 5–14 and in Tables V and VI. The agreement between the experimental results of Sohn *et al.* and both sets of theoretical results is quite good. The trial function with the truncated virtual space is better at energies below 1.0 eV but the results at 0.5 eV must be regarded as fortuitous as experiment yields a Ramsauer minimum at 0.45 eV and the smaller trial function produces a minimum at 0.25 eV. At incident energies of 3.0 eV and above, the agreement between experiment and theory is excellent at scattering angles above 20°. The discrepancy at small scattering angles is due to the slow convergence of the partial-wave expansion. As discussed in the preceding section, the effect of higher partial waves can be included in a partial-wave Born approximation. A spherical (atomic) model is used to investigate these effects by averaging the d-wave eigenphases

TABLE VI. Differential cross sections obtained with (12,39,29) trial functions. Cross-section units are 10^{-16} cm^2.

Angle (deg)	0.5 eV	0.7 eV	1.0 eV	3.0 eV	5.0 eV	7.5 eV
2.000	0.236	0.168	0.041	0.253	2.306	7.146
13.118	0.209	0.147	0.032	0.247	2.025	6.293
30.110	0.114	0.074	0.009	0.305	1.282	3.660
39.000	0.062	0.036	0.006	0.421	1.083	2.457
47.202	0.025	0.012	0.015	0.581	1.115	1.773
56.000	0.004	0.001	0.038	0.776	1.334	1.507
64.317	0.003	0.008	0.072	0.937	1.593	1.547
72.000	0.015	0.025	0.109	1.024	1.755	1.643
81.438	0.042	0.056	0.157	1.016	1.729	1.615
98.562	0.092	0.110	0.221	0.694	1.039	0.911
115.683	0.109	0.133	0.236	0.260	0.274	0.214
132.798	0.091	0.119	0.210	0.091	0.461	0.937
149.890	0.061	0.092	0.171	0.268	1.689	3.215
166.882	0.041	0.071	0.143	0.545	3.015	5.546
178.000	0.037	0.066	0.136	0.631	3.401	6.218

TABLE VII. Integral cross sections from 3 to 10 eV. Cross-section units are 10^{-16} cm^2.

Energy (eV)	Kohn ($l_{max}=5$)	Experiment Ref. [13]	Ref. [14]	Ref. [11]
3	6.264	9.057	7.37	9.25
5	15.940	18.81	18.71	19.0
6	20.575	22.40		22.4
7	23.252	24.56		24.2
8	24.293	25.31		24.7
9	24.248	25.17		24.4
10	23.615	24.68		24.0

occurring in t_2 and e symmetries. A p wave transforms as t_2 in the T_d point group so the p-wave eigenphases are degenerate. The spherical eigenphases are then used in Eqs. (17) and (18) to obtain total and differential cross sections. It is important to bear in mind that the effects of partial waves with $l > 2$ are not converged in the Kohn calculations since $l > 2$ Gaussian basis functions were not included in our calculations. It is computationally very expensive to include enough Gaussian functions to ensure that the Kohn T-matrix elements have converged to the Born results. However, we found the errors introduced by truncating the Gaussian functions at $l = 2$ to be small in the region of the RT minimum, as demonstrated by the results described below. We first ascertained the ability of this spherical model to reproduce the Kohn results. In Fig. 15, the complex Kohn results at 3.0 eV are compared with the spherical model truncated at $l = 2$. As seen in this figure, the averaging introduced in the spherical model does not significantly affect the differential cross section. This model was then used at 0.5 and 3.0 eV to include the effect of higher partial waves in the computation of differential cross sections. The results of these calculations are given in Figs. 16 and 17. The effect of including higher partial waves in the calculations is seen to bring the theoretical cross section into substantial agreement with the experimental results at small scattering angles. The results at 0.5 eV are also improved at large angles where higher partial waves eliminate a dip in the differential cross section. At the energies studied in this work, the effect of including higher partial waves in the integral cross sections was less pronounced, usually amounting to an increase of a few percent from the $l_{max} = 5$ Kohn results.

Integral cross sections were also computed in the region of the broad d-wave resonance. Integral cross sections at incident energies ranging from 3 to 10 eV are given in Fig. 18 and compared to the experiments of Lohmann and Buckmann [13]. A series of experimental results are also presented in Table VII for comparison with our complex Kohn results. The present calculations are in very good accord with the experimental results at energies above 5.0 eV.

IV. CONCLUSION

In this paper we developed a perturbative method of obtaining polarized virtual orbitals. The polarized orbitals were then employed in electron scattering studies of methane at incident energies ranging from 0.2 to 10 eV. Our principal interest was to develop a method capable of yielding reliable cross sections in the region of the Ramsauer-Townsend minimum. A Kohn trial function, based on a polarized-SCF target wave function, was developed and shown to yield electron scattering cross sections that were in excellent agreement with experiments over the full range of incident energies studied.

The difficulty associated with developing a trial scattering function which balances short- and long-range interactions was discussed in some length. The perturbative construction of polarized virtual orbitals from a MCSCF trial function was also considered in this work.

ACKNOWLEDGMENTS

This work was performed under the auspices of the U.S. Department of Energy by the Lawrence Livermore National Laboratory under Contract Number W-7405-Eng-48. C.W. acknowledges support of the National Science Foundation, Grant No. CHE8922836.

[1] A. Jain, Phys. Rev. A **34**, 954 (1986).
[2] A. Jain, Phys. Rev. A **34**, 3707 (1986).
[3] F. A. Gianturco and S. Scialla, J. Phys. B **20**, 3171 (1987).
[4] F. A. Gianturco, A. Jain, and L. C. Pantano, J. Phys. B **20**, 571 (1987).
[5] J. Yuan, J. Phys. B **21**, 2737 (1988).
[6] J. Yuan, J. Phys. B **21**, 3113 (1988).
[7] M. Lima, K. Watari, and V. McKoy, Phys. Rev. A **39**, 4312 (1989).
[8] M. Lima, T. Gibson, W. Huo, and V. McKoy, Phys. Rev. A **32**, 2696 (1985).
[9] C. W. McCurdy and T. N. Rescigno, Phys. Rev. A **39**, 4487 (1989).
[10] H. Tanaka, T. Okada, L. Boesten, T. Suzuki, T. Yamamoto, and M. Kubo, J. Phys. B **15**, 3305 (1982).
[11] J. Ferch, B. Granitza, and W. Raith, J. Phys. B **18**, L445 (1985).
[12] R. Muller, K. Jung, K.-H. Kochem, W. Sohn, and H. Ehrhardt, J. Phys. B **18**, 3971 (1985).
[13] B. Lohmann and S. Buckmann, J. Phys. B **19**, 2565 (1986).
[14] W. Sohn, K.-H. Kochem, K.-M. Scheuerlein, K. Jung, and H. Ehrhardt, J. Phys. B **19**, 3625 (1986).
[15] L. Christophrou, S. Hunter, J. Carter, and R. Mathis, Appl. Phys. Lett. **41**, 147 (1982).

[16] L. Kline, IEEE Trans. Plasma Sci. **PS-10**, 224 (1982).
[17] N. Padial and D. Norcross, Phys. Rev. A **29**, 1742 (1984).
[18] J. O'Connell and N. Lane, Phys. Rev. A **27**, 1893 (1983).
[19] W. Miller and B. Jansen op de Haar, J. Chem. Phys. **86**, 6213 (1987).
[20] C. W. McCurdy, T. N. Rescigno, and B. Schneider, Phys. Rev. A **36**, 2061 (1987).
[21] R. K. Nesbet, *Variational Methods in Electron-Atom Scattering* (Plenum, New York, 1980).
[22] T. N. Rescigno and B. I. Schneider, Phys. Rev. A **37**, 1044 (1988).
[23] B. Schneider and L. Collins, Phys. Rev. A **30**, 95 (1984).
[24] R. K. Nesbet, Phys. Rev. A **20**, 58 (1979).
[25] D. G. Thompson, Proc. R. Soc. London **294**, 160 (1966).
[26] T. O'Malley, L. Spruch, and L. Rosenberg, J. Math. Phys. **2**, 491 (1961).
[27] J. Callaway, Phys. Rev. **106**, 868 (1957).
[28] J. Callaway, R. LaBahn, R. Pu, and W. Duxler, Phys. Rev. **168**, 12 (1968).
[29] A. Temkin, Phys. Rev. **107**, 1004 (1957); **116**, 358 (1959).
[30] A. Temkin and J. Lamkin, Phys. Rev. **121**, 788 (1961).
[31] A. T. Amos and G. G. Hall, Proc. R. Soc. London, Ser. A **263**, 483 (1961).
[32] J. Foster and S. F. Boys, Rev. Mod. Phys. **32**, 300 (1960).
[33] J. Gerratt and I. M. Mills, J. Chem. Phys. **49**, 1719 (1968).
[34] R. N. Camp, H. F. King, J. W. McIver, and D. Mullally, J. Chem. Phys. **79**, 1088 (1983).
[35] M. Page, P. Saxe, G. F. Adams, and B. H. Lengsfield III, J. Chem. Phys. **81**, 434 (1984).
[36] *Geometrical Derivatives of Energy Surfaces and Molecular Properties,* Vol. 166 of *NATO Advanced Study Institute, Series C: Mathematical and Physical Sciences,* edited by P. Jorgensen and J. Simons (Reidel, Dordrecht, 1986).